Advanced MHD models of anisotropy, flow and chaotic fields

M. J. Hole[1], M. Fitzgerald[1], G. R. Dennis[1], S. R Hudson[2], R. L. Dewar[1], G. T. von Nessi[1]

[1]*Res. School of Physics and Eng., Australian National University, ACT, Australia*

[2] *Princeton Plasma Physics Laboratory, PO Box 451, Princeton, NJ 08543, USA*

e-mail address of submitting author: matthew.hole@anu.edu.au

Large scale neutral beam heating, the growing importance of either deliberate or spontaneous equilibrium 3D structure, and the increased diversity, accuracy and resolution of plasma diagnostics have driven more advanced force balance models as well as new approaches to equilibrium reconstruction, such as Bayesian inference techniques [1]. In this work we focus on the development of two MHD force balance models, discuss their constraint to laboratory data, and scope their potential to describe astrophysical phenomena.

EFIT TENSOR is an implementation of the axis-symmetric guiding centre plasma which supports pressure anisotropy and toroidal flow.[2] The free functions are one dimensional poloidal flux functions and all non-linear contributions to the toroidal current density are treated iteratively. The parallel heat flow approximation chosen for the model is that parallel temperature is a flux function and that both parallel and perpendicular pressures may be described using parallel and perpendicular temperatures. In addition to benchmark tests, the code has been applied to MAST data in cases with significant anisotropy.

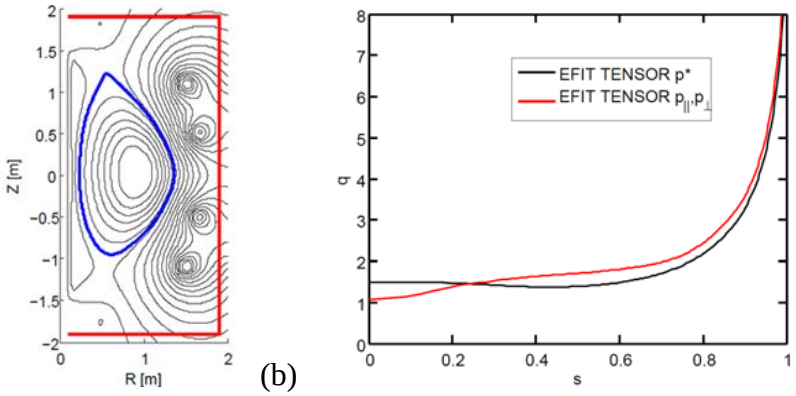

(a) (b)

Figure 1: (a) EFIT TENSOR reconstrution for #29221 at 190ms, (b) EFIT TENSOR *q* profile reconstructions for plasmas with isotropic (p*) and anisotropic ($p_{||}$, $p_{\perp}$) pressure profiles.

Figure 1(a) shows a MAST reconstruction for #29221 at 190ms. This discharge featured 1.6MW of NBI heating with a plasma current of 900kA, and featured a range of MHD activity. Calculations from TRANSP reveal the beam plus thermal population anisotropy is

$p_\perp$ / p|| ~ 1.7. As shown in Fig. 1(b) reconstructions for this discharge that use the isotropic assumption p* = ($p_{||}$+ $p_\perp$)/2 have a significantly different *q* profile to those with $p_\perp$ / p|| ~ 1.7.

We have also developed a single adiabatic compressional stability model in which p|| and $p_\perp$ do joint work. This model, together with the double adiabatic (CGL) model for stability has been implemented in the continuous spectrum code CSMIS and the global stability code MISHKA-A. Figure 2(a) and 2(b) show the difference in the n=1, γ =0 continuum for the isotropic and anisotropic reconstruction, while Figs. 2(c) and (d) show the difference in global mode structure for the two modes. The TAE gap for the anisotropic continuum is much more open than the isotropic case, and the mode peak more inboard than the isotropic case. The implications of this differnt radial structure on wave-particle transport are being currently explored by coupling the EFIT TENSOR and MISHKA-A codes to the wave-particle interaction code HAGIS.

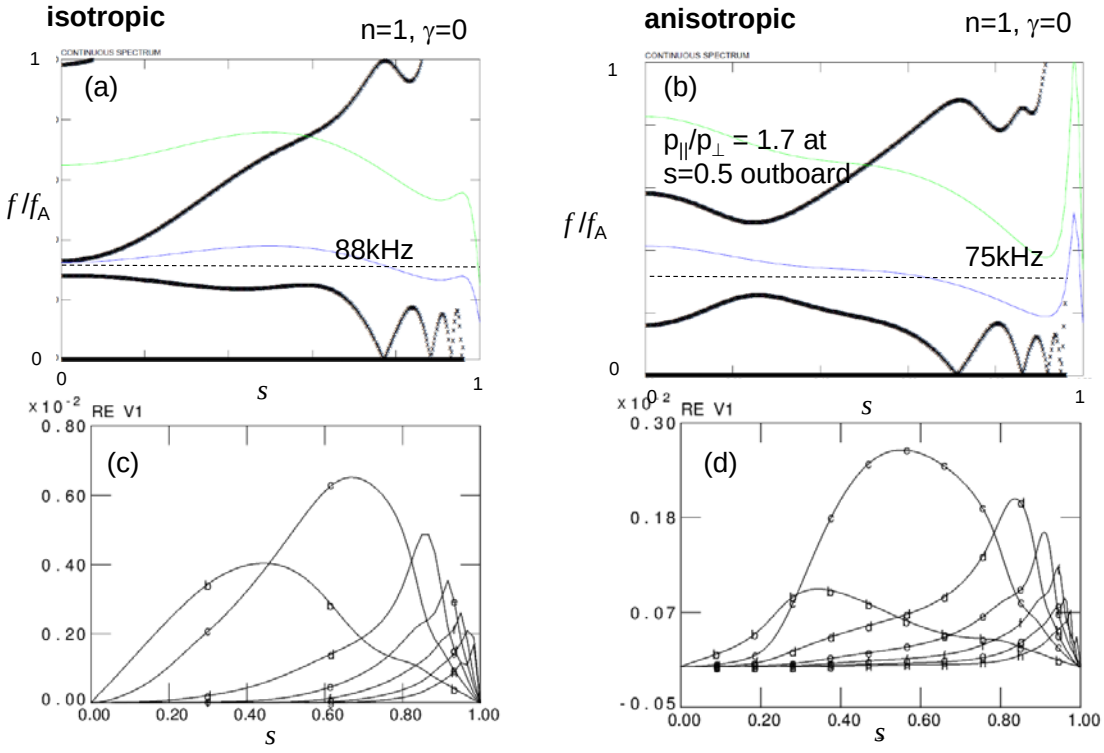

Figure 2: (a) and (b) continuous spectrum for isotropic and ansitropic plasmas. Panels (c) and (d) show global TAE modes for (a) and (b) respectively.

We also report on the development and numerical implementation of multi-region relaxed MHD variational principle MRXMHD, which comprises different Taylor relaxed regions separated by singular currents at ideal MHD interfaces. This model which supports stepped

pressure profiles, enables the resolution of chaotic fields and magnetic islands which occur in toroidal asymmetric plasmas.

In MRxMHD invariant tori act as ideal MHD barriers to relaxation, so that Taylor constraints are localised to subregions. For such a system the energy functional can be written

$$W = \sum_{l=1}^{N} \left(U_l - \mu_l H_l / 2 \right)$$

for a Lagrange multiplier μ_l and with the internal energy U_l and helicity H_l of each region R_i given by

$$U_l = \int_{R_i} \left(\frac{B_l^{\,2}}{2\mu_0} + \frac{P_l}{\gamma - 1} \right) d\tau^3 \qquad H_l = \int_{R_i} (\mathbf{A}_l \cdot \mathbf{B}_l) d\tau^3$$

Solutions of this system of equations provide a Beltrami field, $\nabla \times \boldsymbol{B_l} = \mu_l \boldsymbol{B_l}$ in each plasma region, with a pressure jump condition $[[P_l + B_l^{\,2}/2\mu_0]]=0$ across each interface. We have verified that MRxMHD reproduces MHD in the limit of continuously nested flux surfaces.[3] Extended MRxMHD to include non-zero plasma flow [4]and plasma anisotropy[5], Generalized straight field line coordinates concept to fully 3D plasmas[6], Related helical bifurcation of a Taylor relaxed state to a tearing mode[7,8] and developed techniques to establish pressure jumps a surface can support.[9]

In this work we use the MRxMHD code SPEC[10] to describe the emergence of the quasi-single helicity state in RFX-mod.[11] We have used a two barrier MRxMHD model as a minimal model to describe the formation of double and single helical axis states in the reverse field pinch (RFP). We have compared the plasma energy of the MRxMHD (fully 3D and axisymmetric solutions), as well as ideal MHD (fully 3D and axisymmetric) solutions as a function of barrier position. As the position of the barrier is moved inboard from the plasma edge the fully 3D MRxMHD state diverges from the axisymmetric solution, and has lower energy, showing that the RFP bifurcated state has lower energy (preferred) than the comparable axisymmetric state. This offers an energy principle reason for the formation of single helical axis and double helical axis states. Figure 3 shows experimental[12] and MRxMHD computed Poincare plots for the double helical axis (DAX) and single helical axis (SHAX) states. This MRxMHD computed Poincare plot shows the formation of separate magnetic axes as well as magnetic islands and stochastic regions.

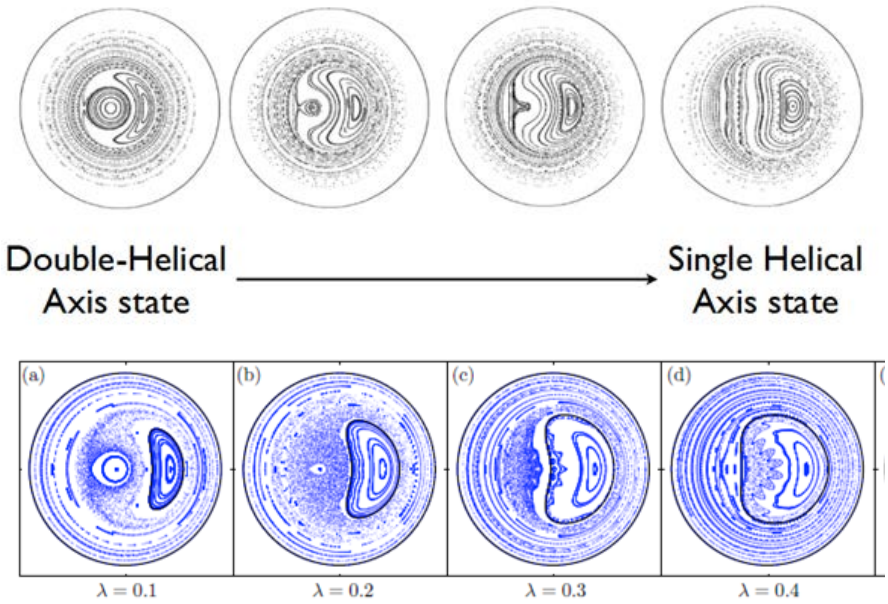

Figure 3: The upper row shows the experimental Poincaré plot with increasing plasma current, while the lower row shows MRxMHD computed Poincaré plots.

In ongoing work we plan to develop SPEC to handle free boundary equilibria, including the vacuum region and external conductors, as well as include toroidal flow.

Acknowledgements:

This work was supported by the Australian Research Council through grant FT0991899, DP110102881, and by the RCUK Energy Programme under Grant No EP/I501045 and the European Communities under the contract of Association between EURATOM and CCFE. The views and opinions expressed herein do not necessarily reflect those of the European Commission.

[1] G T von Nessi, M J Hole, J Svensson, L Appel, Phys. Plas. 19, 013106 (2012).
[2] M. Fitzgerald, L. C. Appel, M. Hole, Nucl. Fusion **53** (2013) 113040
[3] G. Dennis et *al*, Phys. Plas. ,032509, 2013
[4] G.R. Dennis, S.R. Hudson, R.L. Dewar, M.J. Hole, Phys. Plas. **21**, 042501 (2014)
[5] G.R. Dennis, S.R. Hudson, R.L. Dewar, M.J. Hole, Phys. Plas. **21**, 072512 (2014)
[6] R. L. Dewar, S. R. Hudson, A. Gibson, *Plasma Phys. Control. Fusion*, **55,** 014004, 2013
[7] Z. Yoshida and R. L. Dewar , *J. Phys. A: Math. Theor.* **45**, 365502, 2012
[8] M. J. Hole, R. Mills, S. R. Hudson and R. L. Dewar Nucl. Fusion 49 (2009) 065019
[9] M. McGann, ANU PhD thesis, 2013
[10] S. R. Hudson, R. L. Dewar, G. Dennis, M. J. Hole, M. McGann, G. von Nessi and S. Lazerson, Phys. Plasmas 19, 112502, 2012
[11] . R. Dennis, S. R. Hudson, D. Terranova, P. Franz, R. L. Dewar, and M. J. Hole, Physical Review Letters, 111, 055003 (2013)
[12] Fig. 6 of P. Martin et al., Nuclear Fusion 49, 104019 (2009)